Validating the Lower Hybrid Interdigital-line Antenna on MST

M.C. Kaufman, J.A. Goetz, D.R. Burke, A.F. Almagri, S.P. Oliva, J.G. Kulpin

Department of Physics, University of Wisconsin, Madison, WI 53706

Abstract. Lower hybrid current drive has been posited as a means to reduce tearing fluctuations and improve confinement in the reversed field pinch. The third generation interdigital-line antenna has been installed in MST and preliminary testing has been completed. Source power to the antenna has been increased to >220kW in both feed directions. Under vacuum conditions the $n_{\|}$ spectrum is peaked at ~ 7.5 as expected with excellent directionality. External tuning gives a VSWR < 1.3 under most operating conditions; however, power diagnostics on the resonators show a standing wave on the antenna which could affect launch spectrum. Initial plasma parameter surveys show behavior similar to the previous generation antenna. Hard x-ray detectors show flux is toroidally peaked, but still indicative of rf-plasma interaction.

Keywords: LHRF, antenna, interdigital, RFP, MST
PACS: 52.40.Fd, 52.35.Hr, 52.55.Wq

INTRODUCTION

Experimental and theoretical work indicate that anomalous energy and particle transport observed in the reversed field pinch (RFP) is due to tearing fluctuations. These fluctuations can be reduced when parallel current is added to the edge of standard RFP plasmas [1]. Transient inductive techniques (PPCD) [2] have demonstrated significant improvement in energy confinement. Lower hybrid slow waves at $n_{\|} \sim 7.5$ and 800 MHz have been proposed for current drive [3] in the MST RFP.

For the lower hybrid launching structure the traveling wave interdigital-line antenna with capacitively coupled resonators [4] was chosen for MST to satisfy the constraints of both small porthole size and a small vacuum gap between the plasma and wall. Because of the small porthole (and thus power feedthrough) size, multiple antennas must be used for a high power scenario. The third generation (Mk-III) antenna is the next stage in validating the concept of a modular rf system capable of producing 1-2MW of power (the level expected to stabilize tearing fluctuations [3]). Improvements over the second generation (Mk-II) antenna include doubling the size of the coaxial feedthroughs to 4 cm for higher power handling. Modification of impedance matching sections has been made to accommodate the larger feeds as well as reduce the reflection coefficient. The Mk-III antenna has also been more extensively instrumented with a set of power sensing loops embedded in the antenna backplane underneath each resonator on the antenna. Additionally a pair of triple-tip langmuir probes have been installed at either end of the antenna for local density measurements.

CP933, *Radio Frequency Power in Plasmas,* edited by P. M. Ryan and D. A. Rasmussen

For increased source power beyond the 80kW delivered to the second generation antenna, the power supply and pulse-forming network has been upgraded from 27kV/8A for 10 ms to 45kV/17A for 25 ms in a single klystron tube system, with the design goal of a 4-fold increase in source power. The upgraded PFN also has capability of powering two additional klystrons at the same power.

EXPERIMENTAL OBSERVATIONS

The third generation antenna has been able to handle just over 220kW of source power in both feed directions. A Varian-955A 50kW CW klystron is driven at twice its rated voltage and current to produce the rf input power. This power level appears to constitute the present limit of the klystron and power supply rather than the antenna structure.

Extensive modeling with CST Microwave Studio™ was done with the intent of improving the antenna impedance matching sections and with a design goal of a VSWR < 1.1, a major improvement over Mk-II's VSWR of ~ 2 [5]. The antenna, during fabrication, showed an unacceptably high reflection coefficient. Vector voltage measurements showed a large standing wave in the radiating section of the antenna, apparently due to an impedance mismatch. Small modifications of the matching section reduced but did not eliminate the standing wave. Despite the modifications, external tuning was required to achieve a VSWR < 1.3 under most operating conditions.

Figure 1 shows the decay of rf power as the wave travels down the antenna under both vacuum and plasma loading conditions. The measurement is done using the power sensing loops beneath the resonators in the radiating section of the antenna. A model [6] of antenna loading gives an expectation of an exponential damping of the power due to coupling with the plasma as it travels down the antenna. In the vacuum case, damping is due to resistive losses in the antenna structure.

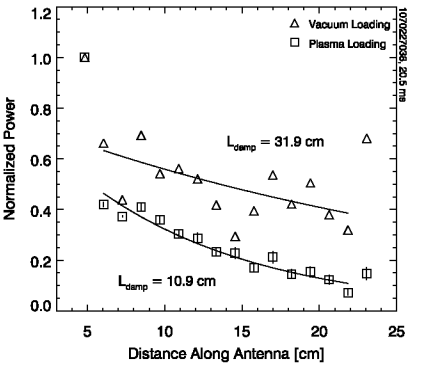

FIGURE 1. Measurement of damping length of rf power flowing down the antenna in vacuum and under plasma loading.

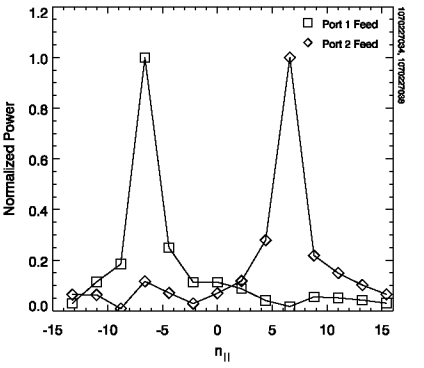

FIGURE 2. Launch $n_{||}$ spectrum of the antenna in both power feed directions during high power pulses.

In both cases in the Figure, the coupling loops under resonators at the edges of the antenna aperture show much higher power than expected from either an exponential damping model or the power flow in the middle of the antenna. These data cannot be explained, but because these artifacts are present in the vacuum loading data, they do not appear to be plasma induced. These resonators are not fully within the radiating section of the antenna, and they are also directly adjacent to the impedence matching sections of the antenna. Either of these conditions may cause the power measurement to be affected, but neither of these explanations has been fully explored.

If the outlying power measurements are disregarded, then a good exponential fit can be made to the data. The vacuum damping length of 31.9 cm corresponds to losses of 0.16dB per resonator. Under the plasma conditions for the data in Figure 1, $L_{damp} = 10.9\,\text{cm}$, giving $\sim$48% of the source power coupled to the plasma.

Vector electronics for each power sensing loop on the antenna as well as a larger number of loops allows measurement of not only the power, but also the relative phasing of the wave as it travels down the antenna structure. Given these, we can calculate the launched $n_{\|}$ spectrum. Figure 2 shows the launch spectrum of two high power shots in both feed directions. As expected, most of the power is peaked around $n_{\|} \sim \pm 7.5$ with good directivity with the port 2 feed and the indication of a small backward wave in the port 1 feed direction

Hard x-ray detection is currently the primary means to detect interaction of the LH wave with the plasma. A movable CdZnTe detector has been placed at various toroidal locations around the machine to measure the intensity of rf-induced x-ray production. In these experiments, we employ 400kA plasmas at densities above $0.75 \times 10^{13}\,\text{cm}^{-3}$ with 160kW of source rf power; for non-rf plasmas with these parameters hard x-rays are almost nonexistent above 10keV. Figures 3 and 4 show the x-ray energy spectra at $-30°$, $0°$, and $30°$ toroidally away from the antenna for both feed directions. Additional measurements were taken at $-150°$ and $90°$ away, but very few counts were observed at these locations.

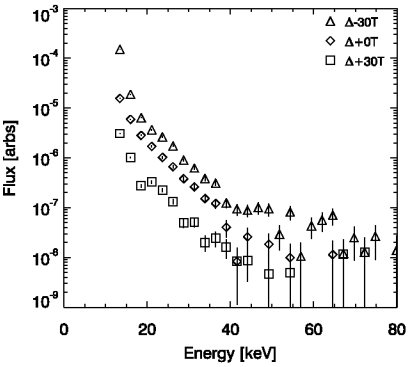

FIGURE 3. Hard x-ray flux vs photon energy for a port 1 feed direction.

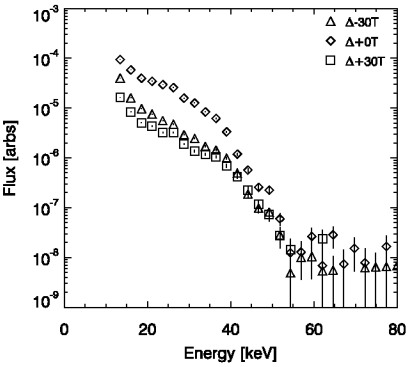

FIGURE 4. Hard x-ray flux vs photon energy for a port 2 feed direction.

In the port 2 direction there is almost an order of magnitude higher flux below 40keV at the antenna location than at toroidal locations 30° away. Port 1's flux is more than an order of magnitude below that of port 2 and we see a higher flux $-30°$ away from the antenna than in front of it.

CONCLUSIONS

The third generation antenna with upgraded power supply has operated with peak source power over 220kW, the present limit of the klystron. Higher power handling may be possible with a higher output klystron or additional klystrons and combiners to deliver more source power. The antenna appears able to handle as much power as we can currently give it, with a low VSWR, making this antenna design promising for a complete modular rf system on MST.

Upgraded power diagnostics on the antenna structure give a better fit for the exponential damping length discounting data from the resonators nearest the impedance matching sections. Phase measurements allow an $n_{\|}$ spectrum to be measured. This launch spectrum shows narrow peaking at $\sim \pm 7.5$ as designed.

The hard x-ray observations indicate significant rf wave interaction with the plasma. The toroidal peaking in the flux suggests that high energy electrons are not being well-confined, but given the low input power and generally poor-confinement plasmas, this is not particularly surprising. That flux is seen away from the antenna as well as x-rays above 50keV implies that x-ray generation is not simply an antenna near-field effect. The shape of the x-ray spectrum, as well as the flux peak locations for each port cannot be properly explained at this time. Future hard x-ray tomography measurements and modeling will hopefully shed more light on these observations.

ACKNOWLEDGMENTS

This work is supported by US DOE Contract DE-FG02-05ER54814

REFERENCES

1. Sovenic, C.R., Prager, S.C., *Nuclear Fusion* **29**, 777 (1999)
2. Sarff, J.S., et. al., *Phys. Rev. Lett.* **72**, 3670 (1994)
3. Uchimoto, E., Cekic, M., Harbey, R.W., et al., *Phys. Plasmas* **1**, 3517 (1994)
4. Matthaei, G.L., *IRE Transactions on Microwave Theory and Techniques*, **Vol MTT-10**, 479 (1962)
5. Goetz, J.A., et al. "Lower Hybrid Antenna Design for MST" *Radio Frequency Power in Plasmas, 16th Topical Conference* (2005)
6. Golant, V.E., Sov. Phys.-Tech. Phys. **16**, 1980 (1972)